

# INFRARED REFLECTANCE INVESTIGATION OF THE STRUCTURE OF $x\text{Sb}_2\text{S}_3 \cdot (1-x)\text{As}_2\text{S}_3$ GLASSES

J.A. KAPOUTSIS<sup>a</sup>, E.I. KAMITSOS<sup>a</sup>, I.P. CULEAC<sup>b</sup> and M.S. IOVU<sup>b</sup>

<sup>a</sup>Theoretical and Physical Chemistry Institute,  
National Hellenic Research Foundation,  
48 Vass. Constantinou Ave., Athens 116 35, Greece

<sup>b</sup>Center of Optoelectronics of the Institute of Applied Physics,  
nr. 1 Academiei Str., Chisinau, MD-2028, Republic of Moldova

## 1. Introduction

Chalcogenide glasses have attracted much attention over the years in light of their technological applications, including infrared transmitting optical elements, acousto-optic and memory switching devices, and materials useful for image creation and storage [1]. In addition, new chalcogenide glass compositions exhibit superionic conducting properties very promising for electrochemical applications [2].

$\text{As}_2\text{S}_3$  is the most extensively studied chalcogenide glass mainly because of its ease of formation, its excellent IR transmission and its resistance to atmospheric conditions and chemicals [3]. Even though As and Sb belong to the same group of the Periodic table,  $\text{As}_2\text{S}_3$  and  $\text{Sb}_2\text{S}_3$  do not display the same glass-forming tendency. Glassy  $\text{Sb}_2\text{S}_3$  is very difficult to form because of the high cooling rates required [4]. However, addition of  $\text{As}_2\text{S}_3$  to  $\text{Sb}_2\text{S}_3$  enhances greatly the glass-forming ability of the latter, and thus, glasses in the mixed system  $\text{Sb}_2\text{S}_3\text{-As}_2\text{S}_3$  can be formed.

It is generally accepted that the three dimensional network of glassy  $\text{As}_2\text{S}_3$  is built of trigonal pyramidal units,  $\text{AsS}_3$ , which are interconnected through As-S-As bridges [5-7]. There is also evidence that the intermediate range order of this glass involves two neighboring pyramids and their shared S-atom, with the correlation length being  $\sim 7\text{\AA}$  [8]. The rearrangement of such coupled pyramids with respect to the neighbors has been used to explain properties such as the reversible photoinduced structural changes [8]. Correspondingly, it has been shown that the basic structural units of glassy  $\text{Sb}_2\text{S}_3$  are the trigonal pyramids  $\text{SbS}_3$  bonded to each other by S atoms [4]. It is of interest to note that the resulting network of glassy  $\text{Sb}_2\text{S}_3$  exhibits lower degree of local disorder around Sb atoms than that of crystalline  $\text{Sb}_2\text{S}_3$  [9].

Despite the general agreement on the structure of glasses  $\text{X}_2\text{S}_3$  ( $\text{X}=\text{As}, \text{Sb}$ ), the structure of glassy materials in the mixed system  $\text{Sb}_2\text{S}_3\text{-As}_2\text{S}_3$  remains controversial. Thus, some authors based on the results of various spectroscopic

techniques, such as EXAFS, XANES, IR and  $^{121}\text{Sb}$ -Mossbauer, propose the random substitution of As by Sb and the creation of mixed As-S-Sb bridges [10-13]. On the other hand, others have interpreted the results of IR [14, 15], XRD [15], crystallization kinetics [16] and optical gap measurements [17] as suggestive of a glass structure consisting of heterogeneous phases of  $\text{As}_2\text{S}_3$  and  $\text{Sb}_2\text{S}_3$  with little or no interactions between them.

It is clear from the above that further work is required to help resolving existing controversies concerning the structure of these mixed chalcogenide glasses. In this paper we present a systematic infrared reflectance study of glass compositions  $x\text{Sb}_2\text{S}_3 \cdot (1-x)\text{As}_2\text{S}_3$  in a wide glass forming region,  $0 \leq x \leq 0.75$ . The purpose of this investigation is twofold; first, to identify the effect of  $\text{Sb}_2\text{S}_3$  addition on the local glass structure, and second, to explore the possibility of formation of mixed As-S-Sb bridges.

## 2. Experimental

Glasses were prepared by melting stoichiometric mixtures of glassy  $\text{As}_2\text{S}_3$  and polycrystalline  $\text{Sb}_2\text{S}_3$  in evacuated (at  $10^{-5}$  Torr) sealed silica ampoules. Melting was performed at  $850^\circ\text{C}$  for *ca* 8 hrs in a rotating furnace in order to ensure homogeneity. Glasses were then obtained by water-quenching the silica tubes. This technique results in  $x\text{As}_2\text{S}_3 \cdot (1-x)\text{Sb}_2\text{S}_3$  glasses in a continuous glass forming region,  $0 \leq x \leq 0.75$ . The color of the obtained glasses varies from red to dark red upon increasing  $\text{Sb}_2\text{S}_3$  content. The bulk glasses were polished to yield flat samples with good quality surfaces appropriate for infrared measurements. It is noted that glassy  $\text{Sb}_2\text{S}_3$  could not be prepared in dimensions suitable for infrared reflectance measurements.

Infrared spectra were recorded in the reflectance mode at near normal incidence ( $11^\circ$  off-normal) on a Fourier-transform vacuum spectrometer (Bruker 113v), using of a high reflectivity Al mirror as reference. A Hg source, a DTGS detector with polyethylene window and five mylar beam splitters with variable thickness ( $3.5\text{-}50\ \mu$ ) were used in the far infrared region in order to measure continuous spectra in the range  $30\text{-}700\ \text{cm}^{-1}$ . Each spectrum represents the average of 200 scans with  $2\ \text{cm}^{-1}$  resolution. The measured reflectivity spectra were analyzed through the Kramers-Kronig inversion technique to obtain the absorption coefficient spectra, as well as the optical and dielectric constants, as described in details elsewhere [18, 19].

## 3. Results and Discussion

Infrared reflection spectra of  $x\text{Sb}_2\text{S}_3 \cdot (1-x)\text{As}_2\text{S}_3$  glasses, with  $\text{Sb}_2\text{S}_3$  contents spanning the entire glass forming region, are presented in Fig. 1. The presented reflectivity spectra are in good agreement with those reported earlier by Kato et al. in the range  $0 \leq x \leq 0.60$  [14]. The spectrum of pure  $\text{As}_2\text{S}_3$  glass ( $x=0$ ) is characterized by a strong

band at  $312\text{ cm}^{-1}$ , a weak feature at  $380\text{ cm}^{-1}$  and a weak and broad band at  $ca\ 100\text{ cm}^{-1}$ . Addition of  $\text{Sb}_2\text{S}_3$  to  $\text{As}_2\text{S}_3$  induces systematic spectral changes. Thus, increasing  $x$  results in the broadening of the main reflection band and its shifting to lower frequencies ( $278\text{ cm}^{-1}$  for  $x=0.75$ ), followed by the progressive weakening of the  $380\text{ cm}^{-1}$  feature.

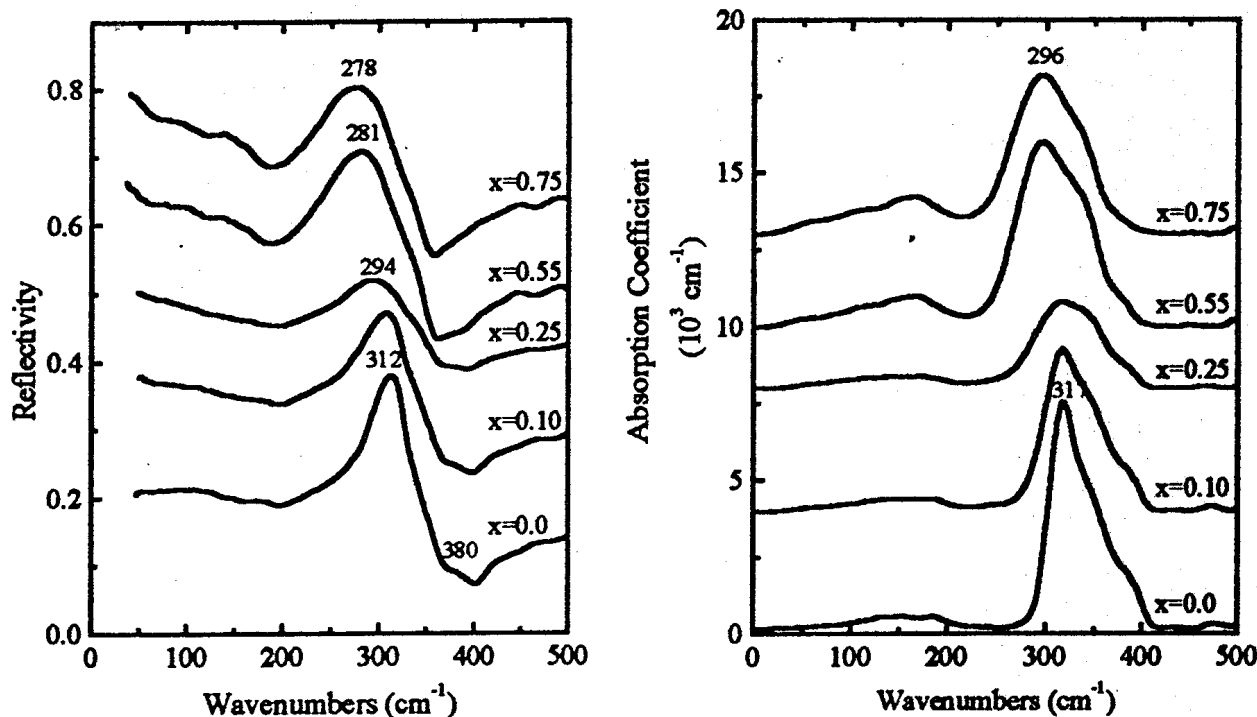


Figure 1 (left). Infrared reflection spectra of  $x\text{Sb}_2\text{S}_3 \cdot (1-x)\text{As}_2\text{S}_3$  glasses. For  $x > 0$ , the spectra have been off-set by 0.175, 0.35, 0.35 and 0.5, respectively, to facilitate comparison.

Figure 2 (right). Absorption coefficient spectra of  $x\text{Sb}_2\text{S}_3 \cdot (1-x)\text{As}_2\text{S}_3$  glasses. Spectra of glasses  $0.1 \leq x \leq 0.75$  have been off-set by 4, 8, 10 and 13 ( $10^3\text{ cm}^{-1}$ ), respectively, to facilitate comparison.

Corresponding changes are observed in the absorption coefficient spectra of these glasses displayed in Fig. 2. The dominant high frequency absorption profile ( $250\text{--}400\text{ cm}^{-1}$ ) becomes broader and shifts to lower frequencies upon increasing  $x\text{Sb}_2\text{S}_3$ . Also, the absorption envelope below  $200\text{ cm}^{-1}$  acquires intensity with  $x$  and peaks eventually at  $ca\ 150\text{ cm}^{-1}$  for  $x=0.75$ .

In order to understand the structural origin of these spectral changes with increasing  $x$  further analysis of the infrared spectra is required. In particular, we focus attention on understanding the evolution of the complex profile  $250\text{--}450\text{ cm}^{-1}$ . This is because absorptions due to stretching vibrations of As-S and Sb-S bands are expected in this frequency range. Thus, we have attempted to deconvolute the high frequency envelope, to assign the resulting component bands and to understand their composition dependence. For this purpose we apply in this work a least-squares-fitting program and

a deconvolution procedure employed previously to study binary and ternary glasses (18-21). In this approach, we use the minimum number of component bands that gives a reasonable agreement between experimental and calculated spectra. The functional form, the frequencies, bandwidths and intensities of component bands are parameters adjustable by the program. The steps of the spectral analysis followed here are described below.

We have started the spectral analysis by considering first the spectrum of the  $\text{As}_2\text{S}_3$  glass ( $x=0$ ). The profile of the 250-400  $\text{cm}^{-1}$  absorption envelope of this glass suggests the existence of at least three component bands (Fig. 2). Indeed, a good fit was obtained with three Gaussian bands, as shown in Fig. 3. The three components, designated by 1As, 2As and 3As, have frequencies 317, 348 and 380  $\text{cm}^{-1}$ , respectively. The assignment of these bands can be made on the basis of the molecular model, proposed for the interpretation of the vibrational spectra of  $\text{As}_2\text{X}_3$  ( $\text{X}=\text{S}, \text{Se}, \text{Te}$ ) glasses [5], and found useful to treat the vibrational spectra of binary glasses such as  $\text{Li}_2\text{S}-\text{As}_2\text{S}_3$  [22]. This model considers the modes of vibrationally decoupled  $\text{AsX}_3$  pyramids and  $\text{As-X-As}$  water-like bridging bonds [5]. Thus, in terms of the molecular model, the stronger band at 317  $\text{cm}^{-1}$  (1As) is assigned to the asymmetric stretching mode,  $\nu_3(\text{E})$ , of  $\text{AsS}_3$  pyramids, while the one at 348  $\text{cm}^{-1}$  (2As) to the symmetric stretching mode,  $\nu_1(\text{A}_1)$ , of the  $\text{AsS}_3$  pyramidal units. Besides those modes,  $\text{AsS}_3$  pyramids exhibit two bending modes,  $\nu_4(\text{E})$  and  $\nu_2(\text{A}_1)$ , which are also infrared active [5] and contribute to the weak absorption in the 100-200  $\text{cm}^{-1}$  frequency range. The high frequency component at 380  $\text{cm}^{-1}$  (3As) is attributed to the asymmetric stretching vibration of  $\text{As-S-As}$  bridges,  $\nu_{\text{as}}(\text{As-S-As})$ . These assignments are consistent with the Raman spectrum of glassy  $\text{As}_2\text{S}_3$ , which shows strong scattering at 343  $\text{cm}^{-1}$  ( $\nu_1$ ), a weaker feature at 312  $\text{cm}^{-1}$  ( $\nu_3$ ) and a shoulder at 373  $\text{cm}^{-1}$  ( $\nu_{\text{as}}(\text{As-S-As})$ ) [6].

The infrared spectrum of a glassy  $\text{Sb}_2\text{S}_3$  film shows the strongest band at 285  $\text{cm}^{-1}$  and a weaker feature at 330  $\text{cm}^{-1}$  [23]. Bernier et al. [24] reported the corresponding bands of amorphous  $\text{Sb}_2\text{S}_3$  dispersed in paraffin at 293  $\text{cm}^{-1}$  and 332  $\text{cm}^{-1}$ . In analogy with  $\text{As}_2\text{S}_3$ , these bands can be attributed to the  $\nu_3$  ( $\sim 290 \text{ cm}^{-1}$ ) and  $\nu_1$  (330  $\text{cm}^{-1}$ ) modes of  $\text{SbS}_3$  pyramidal units. This suggests that consideration of  $\text{SbS}_3$  pyramids is sufficient to explain the infrared spectra of glassy  $\text{Sb}_2\text{S}_3$  in agreement with Ref. [6]. With the above information in mind, and on the basis of the results of deconvolution of the spectrum of  $\text{As}_2\text{S}_3$  ( $x=0$ ), we tried to deconvolute the spectra of mixed  $\text{Sb}_2\text{S}_3-\text{As}_2\text{S}_3$  glasses ( $x>0$ ). As input we used the frequencies and bandwidths of bands 1As, 2As, 3As, as determined for  $x=0$ , plus two additional bands at *ca* 290 and 330  $\text{cm}^{-1}$  to account for the presence of the  $\text{Sb}_2\text{S}_3$  components. With these five bands we could fit the 250-450  $\text{cm}^{-1}$  spectra quite satisfactorily. Using this approach, we found that in all cases the intensity of the 2As band is equal or even higher than that of the 1As band. There is no reason to believe that the symmetric stretching mode,  $\nu_1$  (2As), of  $\text{AsS}_3$  pyramids, which is the strongest band in the Raman spectrum of the  $\text{As}_2\text{S}_3$  glass [6], acquires additional intensity in the infrared spectra of the mixed glasses. Thus, we take this result as suggesting the presence of an additional band close to 2As. When the spectra of mixed glasses were fitted with the input presented above and the consideration of a sixth component at *ca* 350  $\text{cm}^{-1}$ , then the relative

intensities of the resulted 1As and 2As components were similar to that in the spectrum of  $x=0$ . Typical results of deconvolution are shown in Figure 3. Following the assignments for glassy  $\text{Sb}_2\text{S}_3$ , bands 1Sb and 2Sb are attributed to  $\nu_3$  and  $\nu_1$  modes of  $\text{SbS}_3$  pyramids in the mixed network. The origin of the component denoted by 3Sb/As in Fig.3 will be discussed below.

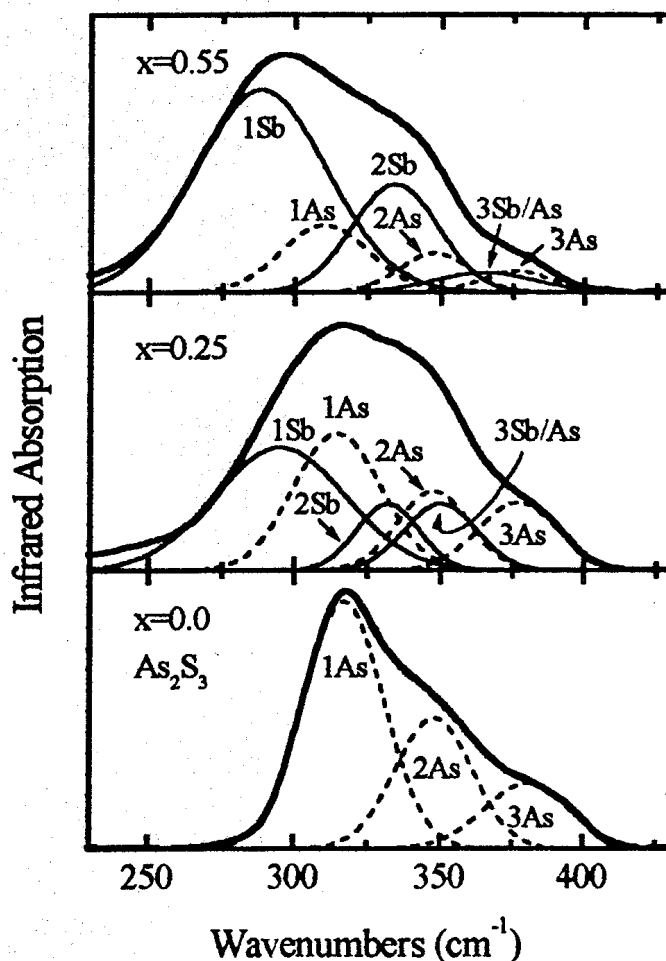
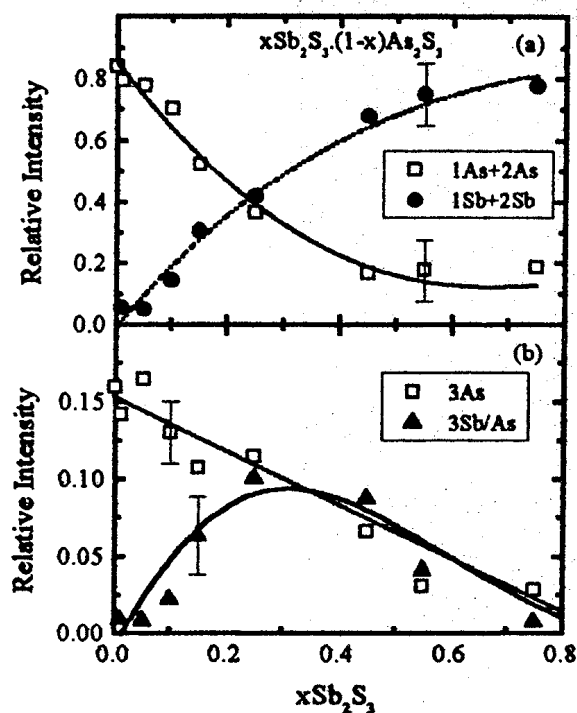
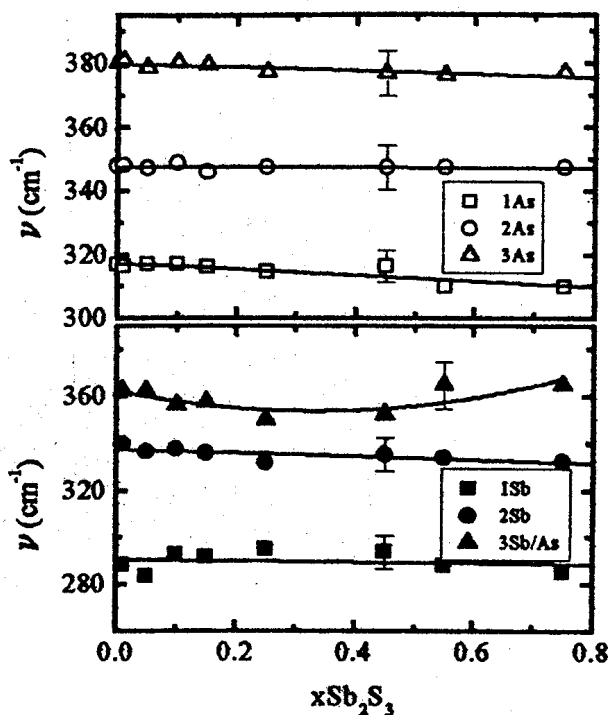


Figure 3. Examples of deconvolution of the higher-frequency envelope 250-450  $\text{cm}^{-1}$  (thick lines) of the infrared spectra of  $x\text{Sb}_2\text{S}_3 \cdot (1-x)\text{As}_2\text{S}_3$  glasses. The simulated spectra are shown by dotted lines.

The frequencies of the component bands are plotted in Figure 4 versus mole fraction of  $\text{Sb}_2\text{S}_3$ . Besides the frequency of band 3Sb/As the rest of them do not display a great variation with composition, suggesting that the structure of the basic building units, i.e. pyramids  $\text{AsS}_3$  and  $\text{SbS}_3$ , is retained in the mixed glasses. Nevertheless, closer examination reveals some systematic trends with  $x$  which deserve our attention. First, it is of interest to note that the difference  $\nu_1(2\text{As}) - \nu_3(1\text{As})$  increases with  $x$ , while  $\nu_1(2\text{Sb}) - \nu_3(1\text{Sb})$  decreases with  $x$ . It was demonstrated by Giehler [6] that the frequency difference  $\nu_1 - \nu_3$  of pyramidal  $\text{XY}_3$  units depends mainly on the value of the pyramidal angle,  $\text{Y-X-Y}$ . In particular,  $\nu_1 - \nu_3$  increases when the angle  $\text{Y-X-Y}$  decreases. On this basis, the observations made above indicate that the pyramidal angle for both pyramids,  $\text{AsS}_3$  and  $\text{SbS}_3$ , decreases in the mixed glass with respect to

the values they have in pure  $\text{As}_2\text{S}_3$  and  $\text{Sb}_2\text{S}_3$  glasses. Second, it is observed that the frequency of the 3As band,  $\nu_{\text{as}}(\text{As-S-As})$ , decreases with  $x\text{Sb}_2\text{S}_3$ . The implication of



*Figure 4 (left).* Composition dependence of the frequencies of the component bands resulted from the deconvolution of the  $250\text{--}450\text{ cm}^{-1}$  absorption envelope (see fig. 3) of  $x\text{Sb}_2\text{S}_3 \cdot (1-x)\text{As}_2\text{S}_3$  glasses. Lines are least-squares fitting.

*Figure 5 (right).* Relative intensities of component bands versus  $\text{Sb}_2\text{S}_3$  content. Lines are drawn to guide the eye. For details see text.

this trend can be understood in terms of the following formula which gives the frequency of the asymmetric stretching vibration of X-Y-X bridges [25]:

$$\nu_{\text{as}}^2 = \left[ \frac{1}{4\pi^2 c^2} \right] \left[ \frac{1}{m_X} + \frac{2}{m_Y} \sin^2 \alpha \right] k_r \quad (1)$$

where  $m_X$ ,  $m_Y$  are the masses of atoms X and Y, respectively,  $k_r$  is the force constant of bond X-Y,  $2\alpha$  is the angle X-Y-X and  $c$  is the speed of light. If the force constant of the bond As-S does not change upon mixing, then the observed trend of  $\nu_{\text{as}}(\text{As-S-As})$  (3As) suggests, in term of Eq. (1), the decrease of the As-S-As angle upon increasing  $x\text{Sb}_2\text{S}_3$ . The variation with  $x$  of the frequency of the 3Sb/As band is considered below in connection with the composition dependence of its relative intensity.

Figure 5 shows the composition dependence of the relative intensities of the component bands in the  $250\text{--}450\text{ cm}^{-1}$  envelope. The intensities of bands 1As and 2As, as well as those of 1Sb and 2Sb, have been considered together (Fig. 5(a)), since they both originate from intramolecular vibrations of the  $\text{XS}_3$  pyramids ( $X=\text{As}, \text{Sb}$ ). The

relative intensity of bands attributed to  $\text{AsS}_3$  pyramids decreases monotonically with  $x\text{Sb}_2\text{S}_3$ , while the relative intensity of bands assigned to  $\text{SbS}_3$  pyramids increases, as expected. It is noted though that the intensity of bands  $1\text{Sb}+2\text{Sb}$  relative to that of  $1\text{As}+2\text{As}$  is considerably higher than would be expected from the mole fraction of  $\text{Sb}_2\text{S}_3$  alone. The observed differences can be explained if we consider the changes of dipole moment involved in the vibrations of the X-S bonds. Indeed, it has been shown that the effective charge involved in Sb-S bonding is considerably higher than that involved in As-S bonding [6, 14].

The relative intensity of band  $3\text{As}$ , characteristic of As-S-As bridges, decreases monotonically with  $x$  (Fig. 5(b)). This is consistent with a progressive destruction of such bridges as the  $\text{As}_2\text{S}_3$  content in the mixed system decreases. The relative intensity of band  $3\text{Sb}/\text{As}$  displays a non-linear dependence on  $x$ , passing through a maximum value at  $x \approx 0.35$  (Fig. 5(b)). Since the probability for creating mixed As-S-Sb bridges would be maximized at  $x \approx 0.5$ , the composition dependence of the relative intensity of  $3\text{Sb}/\text{As}$  band is suggesting its assignment to  $\nu_{\text{as}}(\text{As-S-Sb})$ .

According to Eq. (1),  $\nu_{\text{as}}(\text{As-S-Sb})$  would depend on an effective force constant,  $k_{\text{eff}}$ , and on an effective bond angle, As-S-Sb, both of which could be composition dependent. As shown previously [6]  $k_{\text{As-S}} > k_{\text{Sb-S}}$ , therefore  $k_{\text{eff}}$  is expected to decrease with  $x$ . On the other hand, the bridging angle, X-S-X, was estimated to be  $99.5^\circ$  in the  $\text{As}_2\text{S}_3$  glass and  $100.7^\circ$  in  $\text{Sb}_2\text{S}_3$  glass [4]. Thus, the effective angle As-S-Sb would increase with  $x$ . The combined effect of both factors could lead, according to Eq. (1), to a minimum value of  $\nu_{\text{as}}(\text{As-S-Sb})$  with composition. The composition dependence of the frequency of the  $3\text{Sb}/\text{As}$  band (Fig. 4) is in accord with the proposed assignment.

The infrared results discussed above are supportive of the models proposing the random substitution of As by Sb, rather than the formation of heterogeneous  $\text{As}_2\text{S}_3$  and  $\text{Sb}_2\text{S}_3$  phases connected at the interfaces via mixed As-S-Sb bridges. If the latter proposition were true then one would expect that at least the intramolecular vibrations of  $\text{XS}_3$  pyramids, in the two different microphases, would be independent of composition. However, this was not observed in the present work. In particular, the systematic variations with  $x$  of especially the  $\nu_1$  and  $\nu_3$  modes of the pyramids (Fig. 4), is indicating considerable neighboring of the  $\text{AsS}_3$  and  $\text{SbS}_3$  pyramids.

#### 4. Conclusions

The structure of glasses in the mixed system  $x\text{Sb}_2\text{S}_3 \cdot (1-x)\text{As}_2\text{S}_3$  has been investigated in a wide composition range ( $0 \leq x \leq 0.75$ ) employing infrared reflectance spectroscopy. The high frequency profiles ( $250-400 \text{ cm}^{-1}$ ) of the absorption coefficient spectra were deconvoluted into component bands in order to study the composition dependence of the glass structure. The main components of the deconvoluted spectra were understood on the basis of the intramolecular vibrations of trigonal  $\text{AsS}_3$  and  $\text{SbS}_3$  pyramids. While the structure of such pyramids is basically retained, it was found that the pyramidal S-X-S angle (X=As, Sb) decreases upon mixing. The destruction of As-S-As

bridges with increasing  $\text{Sb}_2\text{S}_3$  content was found to be accompanied by the creation of mixed As-S-Sb bridges with their relative abundance showing maximum value at  $ca\ x=0.35$ . It was concluded that the composition dependence of the frequencies and relative intensities of the component bands found in this work is suggestive of a considerable mixing of  $\text{AsS}_3$  and  $\text{SbS}_3$  pyramids, rather than of the formation of separate  $\text{As}_2\text{S}_3$  and  $\text{Sb}_2\text{S}_3$  microphases.

**Acknowledgment.** *A grant from the NATO Special Fellowships Program supported the stay of I.P.C. at NHRF and made this collaborative work possible.*

## 5. References

1. Seddon, A.B. (1995) Chalcogenide glasses: a review of their preparation, properties and applications, *J. Non-Crystalline Solids* **184**, 44-50 and references therein.
2. Elliott, S.R. (1991) Chalcogenide glasses, in R.W. Kahn, P. Haasen and E.J. Kramer (eds), *Materials Science and Technology*, VCH, Weinheim, Vol. 9, Glasses and Amorphous Materials, J. Zarzycki (ed.), pp. 375-454.
3. Rawson, H. (1967) *Inorganic Glass-Forming System, Non-Metallic Solids*, Academic Press, London.
4. Cervinka, L., and Hruby, A. (1982) Structure of amorphous and glassy  $\text{Sb}_2\text{S}_3$  and its connection with the structure of  $\text{As}_2\text{X}_3$  arsenic-chalcogenide glasses, *J. Non-Crystalline Solids* **48**, 231-264.
5. Lucovsky, G. (1971) Optic modes in amorphous  $\text{As}_2\text{S}_3$  and  $\text{As}_2\text{Se}_3$ , *Physical Review B* **6**, 1480-1489 and references therein.
6. Giehler, M. (1981) The effect of short-range order on the vibrational spectra of 3:2 coordinated chalcogenide glasses, *Physica Status Solidi (b)* **106**, 193-205.
7. Itoh, S., and Fujiwara, T. (1982) Vibrational properties of  $\text{As}_2\text{S}_3$  glass, *J. Non-Crystalline Solids* **51**, 175-186.
8. Paesler, M.A., and Pfeiffer, G. (1991) Modeling the structure and photostructural changes in amorphous arsenic sulfide, *J. Non-Crystalline Solids* **137-138**, 967-972.
9. Dalba, G., Fornasini, P., Giunta, G., and Burattini, E. (1989) XRD and EXAFS study of the local structure in some non-crystalline Sb-S compounds, *J. Non-Crystalline Solids* **107**, 261-270.
10. El Idrissi Raghni, M.A., Lippens, P.E., Olivier-Fourcade, J., and Jumas, J. (1995) Local structure of glasses in the  $\text{As}_2\text{S}_3$ - $\text{Sb}_2\text{S}_3$  system, *J. Non-Crystalline Solids* **192-193**, 191-194.
11. Durand, J.M., Lippens, P.E., Olivier-Fourcade, J., and Jumas, J.C. (1995) A structural study of glasses in the  $\text{As}_2\text{S}_3$ - $\text{Sb}_2\text{S}_3$ - $\text{Ti}_2\text{S}$  system, *J. Non-Crystalline Solids* **192-193**, 364-368.



12. Durand, J.M., Lippens, P.E., Olivier-Fourcade, J., Jumas, J.C., and Womes, M. (1996) Sb LIII-edge XAS study of the ternary system  $\text{As}_2\text{S}_3\text{-Sb}_2\text{S}_3\text{-Ti}_2\text{S}_3$ , *J. Non-Crystalline Solids* **194**, 109-121.
13. Bychkov, E., and Wortmann, G. (1993)  $^{121}\text{Sb}$  Mossbauer study of insulating and ion-conducting antimony chalcogenide-based glasses, *J. Non-Crystalline Solids* **159**, 162-172.
14. Kato, M., Onari, S., and Arai, T. (1983) Far infrared and Raman spectra in  $(\text{As}_2\text{S}_3)_{1-x}(\text{Sb}_2\text{S}_3)_x$  glasses, *Japanese J. Applied Physics* **22**, 1382-1387.
15. Kawamoto, Y., and Tsuchihashi, S. (1969) The properties and structure of glasses in the system  $\text{As}_2\text{S}_3\text{-Sb}_2\text{S}_3$ , *Yogyo-Kyokai-Shi* **77**, 328-335.
16. White, K., Crane, R.L., and Snide, J.A. (1988) Crystallization kinetics of As-Sb-S glass in bulk and thin film form, *J. Non-Crystalline Solids* **103**, 210-220.
17. Tichy, L., Triska, A., Frumar, M., Ticha, H., and Klikorka, J. (1982) Compositional dependence of the optical gap in  $\text{Ge}_{1-x}\text{S}_x$ ,  $\text{Ge}_{40-x}\text{Sb}_x\text{S}_{60}$  and  $(\text{As}_2\text{S}_3)_x(\text{Sb}_2\text{S}_3)_{1-x}$  non-crystalline systems, *J. Non-Crystalline Solids* **50**, 371-378.
18. Kamitsos, E.I., Patsis, A.P., Karakassides M.A., and Chryssikos, G.D. (1990) Infrared reflectance spectra of lithium borate glasses, *J. Non-Crystalline Solids* **126**, 52-67.
19. Kamitsos, E.I., Kapoutsis, J.A., Chryssikos, G.D., Taillades, G., Pradel, A., and Ribes, M. (1994) Structure and optical conductivity of silver thiogermanate glasses, *J. Solid State Chemistry* **112**, 255-261.
20. Kamitsos, E.I., Kapoutsis, J.A., Jain, H., and Hsieh, C.H. (1993) Vibrational study of the role of trivalent ions in sodium trisilicate glasses, *J. Non-Crystalline Solids* **171**, 31-45.
21. Kamitsos, E.I., Kapoutsis, J.A., Chryssikos, G.D., Hutchinson, J.M., Pappin, A.J., Ingram, M.D., and Duffy, J.A. (1995) Infrared study of AgI containing superionic glasses, *Physics and Chemistry of Glasses* **36**, 142-150.
22. Shastry, M.C.R., Couzi, M., Levasseur, A., and Menetrier, M. (1993) Raman spectroscopic studies of  $\text{As}_2\text{S}_3$  and  $\text{Li}_2\text{S-As}_2\text{S}_3$  glasses, *Philosophical Magazine B* **68**, 551-560.
23. Droichi, M.S., Vaillant, F., Bustarret, E., and Jousse, D. (1988) Study of localized states in amorphous chalcogenide  $\text{Sb}_2\text{S}_3$  films, *J. Non-Crystalline Solids* **101**, 151-155.
24. Barnier, S., Guittard, M., Julien, C., and Chilouet, A. (1993) Study of the antimony environment in gallium-antimony-sulphur glasses-Phase diagram and infrared absorption investigations, *Materials Research Bulletin* **28**, 399-405.
25. Herzberg, G. (1945) *Infrared and Raman spectra of polyatomic molecules*, New York, Van Nostrand, Chapter II.